Renal Fibrogenesis and Platinum Compounds in a Rat Model: A Novel Pt (II) Complex *vs*. Cisplatin

CARLA FENOGLIO[1], FEDERICA ALBICINI[1], SANDRA ANGELICA DE PASCALI[2], GLORIA MILANESI[1], MARCO FUMAGALLI[1], DANILO MIGONI[2], FRANCESCO PAOLO FANIZZI[2] and GRAZIELLA BERNOCCHI[1]

[1]*Department of Biology and Biotechnology, University of Pavia, Pavia, Italy;*
[2]*Department of Biotechnology and Environmental Science, University of Salento, Lecce, Italy*

Abstract. *Background/Aim: A new platinum compound, (Pt(O,O'-acac)(γ-acac)(DMS)) (PtAcacDMS), has been shown to possess higher cytotoxic activity than cisplatin on several cancer and chemoresistant cell lines. The aim of the present study was to compare the nephrotoxic effects - particularly renal fibrogenesis- of PtAcacDMS and cisplatin in rats after the subcutaneous administration of a single dose (5 mg/Kg b.w., s.c.) of either compound to ten-day-old rats. Materials and Methods: Control and treated rats were killed 1 day (PD11), 7 days (PD17), 21 days (PD31) and 40 days (PD50) after the injection. Kidneys were processed for light and electron microscopy, and platinum determination. Antibodies against E-cadherin (E-cad), vimentin (VIM) and α-smooth muscle actin (αSMA) were used to identify epithelial and mesenchymal cells. Results and Conclusion: Cisplatin produced progressive cortical fibrotic lesions displaying a variable number of VIM-positive tubules and interstitial αSMA-positive cells around. By contrast, PtAcacDMS induced a minimal number of histopathological changes, which declined in the adult samples, while the renal platinum content was generally higher after PtAcacDMS than after cisplatin. The present experimental model was proven suitable to investigate the occurrence of epithelial-mesenchymal transition (EMT) in renal fibrogenesis induced by the platinum-based compounds.*

Cisplatin (*cis* diamminedichloroplatinum(II)) is one of the most widely used chemotherapeutic drugs for several types of malignancies in adults and children. However, the benefits of this anti-neoplastic agent are compromised by acquired resistance to cisplatin by cancer cells (1) and severe side-effects, such as neurotoxicity, nephrotoxicity, ototoxicity, myelosuppression and emetogenicity. Among the most frequent complications caused by cisplatin administration in humans and experimental animals, tubulointerstitial fibrosis ranks as one of the most serious as it leads to progressive and irreversible failure of the renal functions (2). In particular, certain reports indicate that cisplatin nephrotoxicity occurs in 25-30% of patients after a single dose of the drug (3).

Interestingly, age-related differences in kidney injuries following administration of cisplatin have been reported in both animals and humans pointing to age as a potential risk factor for cisplatin nephrotoxicity (4-9). Yet, progressive renal fibrosis in experimental animals after cisplatin treatment has been found as a long-term side effect leading to severe kidney impairment (10-12).

The recently synthesized platinum complex (Pt(O,O'-acac)(γ-acac)(DMS)) (PtAcacDMS), on the other hand, could offer an attractive alternative to cisplatin treatment. Containing two acetylacetonate ligands, (one O,O'-chelate and the other sigma-linked by methionine in the gamma position) and dimetylsulphide (DMS) in the metal coordination sphere (13, 14), this compound has demonstrated high cytotoxicity in different cancer cell lines, including the cisplatin-resistant breast cancer cell line MCF-7 while being inactive on the normal cell line MCF-10A. In contrast to cisplatin, which binds primarily to DNA-forming platinum adducts, the main targets of PtAcacDMS seem to be amino acid residues of proteins and enzymes involved in apoptotic induction, thus acting as a compound with non-genomic targets (15, 16). Importantly, PtAcacDMS enters cells rapidly and its cell content and cytotoxic effects are 10-times higher than cisplatin's (16).

Previous *in vivo* neurotoxicity studies on neonatal rats (17-19) have found that, compared to cisplatin, PtAcacDMS produces less severe changes in fundamental events of neuroarchitecture development of the cerebellum.

In the current study, we investigated the *in vivo* nephrotoxic effects of a single dose of either cisplatin or

Correspondence to: Dr. Carla Fenoglio, Dipartimento di Biologia e Biotecnologie, Università di Pavia, Via Ferrata, 9 Pavia, I- 27100 Pavia, Italy. Tel: +39 0382 986315, Fax: +39 0382 986406, e-mail: fenoglio@unipv.it

Key Words: Cisplatin, (Pt(O,O'-acac)(γ-acac)(DMS)), renal fibrogenesis, epithelial-mesenchymal transition.

PtAcacDMS during rat postnatal development with particular attention to the occurrence of renal fibrosis. We examined renal morphology at early and late stages of platinum compound treatment. The progression of renal lesions was determined immunohistochemically by following the distribution pattern of E-cadherin (E-cad), vimentin (VIM) and α-smooth muscle actin (αSMA) within the renal parenchyma of control and treated rats at different ages. Changes in their expression could denote epithelial-mesenchymal transition (EMT), a process that is implicated in renal fibrogenesis as stems from emerging evidence (20). Renal accumulation of platinum was also measured in all samples.

Materials and Methods

Animal care and treatment. Female Wistar rats and their neonatal offspring (Charles River Laboratories, Calco Lecco, Italy) were housed in plastic cages, maintained in controlled conditions (22˚C with a 12 h light-dark cycle) and provided with rat chow and tap water *ad libitum*.

Ten-day-old neonatal rats (postnatal day 10, PD10), weighing 16-23 g, were given a single subcutaneous injection of either cisplatin (0.5 mg/ml; Teva Pharma, Assago Milano, Italy) or PtAcacDMS at a dose of 5 mg/kg b.w. Each solution was prepared immediately before use. The dose, corresponding to a therapeutic dose (21), was based on our previous experimental studies (17, 18). Before necropsy, each animal was anesthetized with an intraperitoneal injection of 35% chloral hydrate (100 μl/100 g b.w.; Sigma, St. Louis, MO, USA). Treated animals were killed 1 day (PD11), 7 days (PD17), 21 days (PD31) and 40 days (PD_{50}) after the injection. These end-points were selected to compare the nephrotoxic effects on developing and mature kidneys. Treated groups of animals (n=6) and control animals (n=4) were killed at each of four examination points. Body weights of the animals were measured.

Animal care and experimental procedures of this study were carried out in compliance with Italian institutional guidelines (art.4 and 5 of DDL 116/92). All efforts were made to minimize the number of animals used and their suffering.

Sample processing. Kidneys were removed bilaterally from each animal and were sagittally hemi-sectioned through the hilus for histopathology. Pieces of both halves of each kidney were either fixed by immersion for 24 h in 2% paraformaldehyde (Sigma Chemical Co., St. Louis, MO, USA) in 0.1 M phosphate buffer pH 7.4, embedded in Paraplast wax and sectioned at 5 μm thickness; or fixed by immersion for 3h in ice-cold 1.5% glutaraldehyde (Polysciences Inc., Warrington, PA, USA) in 0.05M cacodylate buffer pH 7.4 and post-fixed with 1% OsO_4 (Sigma Chemical Co.) in the same buffer for 2 h at 4˚C, dehydrated in graded series of ethanol, embedded in Epon 812 and sectioned with a C. Reichert OMU3 ultramicrotome (Reichert, Vienna, Austria) to obtain semi-thin sections (1μm thick) and ultrathin sections (600 Å thick).

Platinum determination. Frozen pieces of kidney from treated and untreated rats were lyophilized using a LIO 5P lyophilizer (Cinquepascal, Milan, Italy). The material collected was then aliquoted and stored at –80˚C until analysis. The total amount of platinum uptake was performed at CIRCMSB (Consorzio Interuniversitario di Chimica dei Metalli nei Sistemi Biologici, Bari, Italy) by Inductively Coupled PlasmaMass Spectrometry (ICP-MS; Varian ICP-MS 820-MS with autosampler/autodiluter SPS3). The total Pt amount was determined in acid digested mouse kidney, applying the digestion procedure used for organic matrices (22). The data obtained were expressed in μg Pt/kg dry tissue.

Tissue morphology and number of glomeruli. For light microscopy, Paraplast-embedded sections were stained either with hematoxylin-eosin (H&E) or Periodic Acid-Schiff (PAS) reaction and Epon-embedded semi-thin sections were stained with 1% Toluidine Blue (TB).

Histological sections were used to count the number of glomeruli in control and treated adult rats at PD50. The counts were made under the light microscope (objective x40) by an observer blinded to the treatment group. For each untreated control (n=4) and treated rat (n=4 with cisplatin, n=4 with PtAcacDMS), 6 sections (random areas every 50 μm approximately for each section) were examined. Results were recorded on Microsoft Office Excel Software spreadsheets and are reported as the mean±standard deviation. The statistical significance of any differences between control and treated animals was determined by the Student's *t*-Test.

For electron microscopy, ultrathin sections were contrasted with uranyl acetate and Reynold's lead citrate solution. The specimens were then observed under a Zeiss EM 300 electron microscope (Carl Zeiss SpA, Oberkochen, West Germany) at 80 Kv.

Immunohistochemistry. For immunohistochemical analysis, all sections were run simultaneously under identical conditions. They were dewaxed in xylene and rehydrated in a decreasing ethanol series. The endogenous peroxidases were suppressed by incubation of sections with 3% H_2O_2 in 10% methanol in phosphate-buffered saline (PBS; Sigma) for 20 min at room temperature. For antigen retrieval, deparaffinized sections were pretreated in 10 mM TET-buffer (pH 9) by microwave heating for 10 min; they were then incubated in a dark moist chamber with each primary antibody diluted in PBS: anti-E-Cad (1:100, Mouse monoclonal, M3612, Dako, North America, CA, USA at room temperature for 60 min), anti-VIM (ready to use, Mouse monoclonal, IS630, Dako, Glostrup, Denmark, at 4˚C overnight), anti-αSMA (ready to use, Mouse monoclonal, IS611, Dako, Glostrup, Denmark, at 4˚C overnight).

All sections were briefly washed twice with PBS at room temperature. Reactions were revealed (30 min at room temperature) with the peroxidase-conjugated EnVision+System HRP (K4000, anti-mouse; Dako, North America, CA, USA), using 3,3-diaminobenzidine (DAB; Dako, North America, CA, USA) as chromogen substrate. The sections were briefly counterstained with haematoxylin, dehydrated and mounted with Entellan. Negative controls were obtained both by omitting the primary antibody and by replacing the primary antibody with non-immunized mouse serum; positive controls were performed as suggested by the manufacturer.

All slides were observed and with a Zeiss Axioskop 2 Plus light microscope equipped with Differential Interference Contrast (DIC) system (Carl Zeiss Microimaging, Jena, Germany) and then photographed with a Canon EOS 1100D utilized at 6 megapixel (Tokyo, Japan).

Immunoreactivity of control and treated samples were semi-quantitatively scored by two independent observers as follows: –,

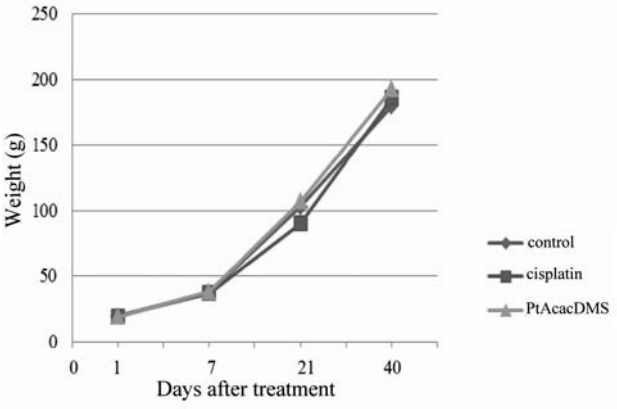

Figure 1. *Body weight of control and treated animals.*

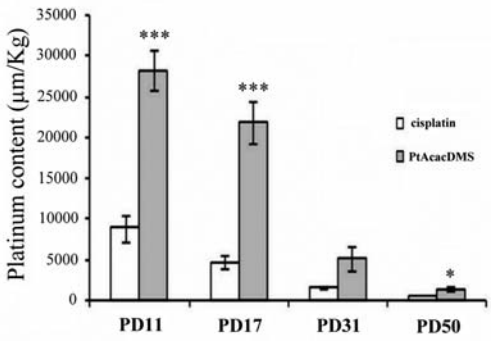

Figure 2. *Kidney platinum content after cisplatin and PtAcacDMS treatment: the bar charts show that, at each stage, the kidney platinum content after PtAcacDMS treatment was significantly higher than after cisplatin. Values are expressed as the mean±S.D. The significance was tested by the Student's t-test. *p<0.05, **p<0.01, ***p<0.001.*

negative; +/– very weak staining; +, weak staining; ++, moderate staining; +++, intense staining.

Results

Mortality and body weight. At the dose used in the study, no deaths occurred in either of the treated groups. As shown in Figure 1, no significant changes in group mean body weights were observed at any study stage. The body weights ranged from 17-24 g at PD11; from 34-41 g at PD17; from 90-196 g at PD31 and from 179-192 g at PD50.

Kidney platinum content. Kidney platinum content in PtAcacDMS-treated samples was considerably higher with respect to cisplatin-treated samples at each stage of development and was particularly significant at PD11 and PD17 (Figure 2). Of note, higher platinum content was still evident in PtAcacDMS samples at PD31 and PD50. In controls, platinum content was practically nil (data not shown).

Histopathology of the kidneys. Sections of rat kidney of all ages stained with both H&E and PAS reaction and semi-thin sections were examined by light microscopy. During the neonatal phase, special attention was given to the nephrogenic zone within the cortex; particularly interesting samples were then examined for their ultrastructure.

In neonatal controls, a number of developing renal corpuscles and elongated tubules of the medullary rays were detected within the cortex of the renal parenchyma (Figure 3A). The tubules were separated from each other by interstitial cells of fusiform profile, especially in the medullary zone. At PD31 and PD50, the control samples exhibited typical mature renal parenchyma with numerous nephrons. After PAS reaction (Figure 3B), a thin basal lamina was seen lining the glomeruli and the renal tubules; proximal tubules exhibited regularly stained brush borders. In comparison with neonates, the interstitial cells were less numerous, especially in the cortex as compared to the medulla.

Generally, the cortical nephrogenic zone in neonatal PtAcacDMS-treated rats showed similarity with control samples having some immature nephrons present; the elongated medullary rays were supported by a regular arrangement of peritubular interstitial cells (Figure 3C). At PD17, rare altered renal tubules were seen within the cortex (Figure 3C inset). Of particular note was a semi-thin section showing a single epithelial cell in the act of migrating out of a dilated tubule section towards the surrounding fibrotic area (Figure 3D). In the adult samples, both the cortex and the medulla appeared most similar to controls (Figure 3E and F).

Tubulointerstitial alterations were noticed in the renal parenchyma of cisplatin-injected rats, the degree of which varied with age. As compared to controls, cisplatin induced early changes in neonatal rats affecting primarily the outer renal cortex where some dilated tubules were noted (Figure 4A). At PD31 and most notably at PD50, the PAS reaction revealed recurrent dilated tubules rimmed with flattened epithelia and variable numbers of surrounding interstitial cells (Figure 4B). In both semi-thin and ultrastructural sections of adult samples, injured tubules displayed irregular, spindle-shaped or flattened epithelial cells and thickened basal lamina below; sporadic detaching cells in the lumen were observed (Figure 4C). Infiltrating cells were occasionally seen beneath the epithelial cells of altered tubules at both light and electron microscopy (Figure 4D). Noteworthy was the observation of single epithelial cell migrating through the plane of an altered tubule toward the interstitium at both light (Figure 4E) and electron microscope (Figure 4F).

Number of glomeruli. Glomeruli count was performed at PD50, *i.e.* upon nephrogenesis completion. There was a

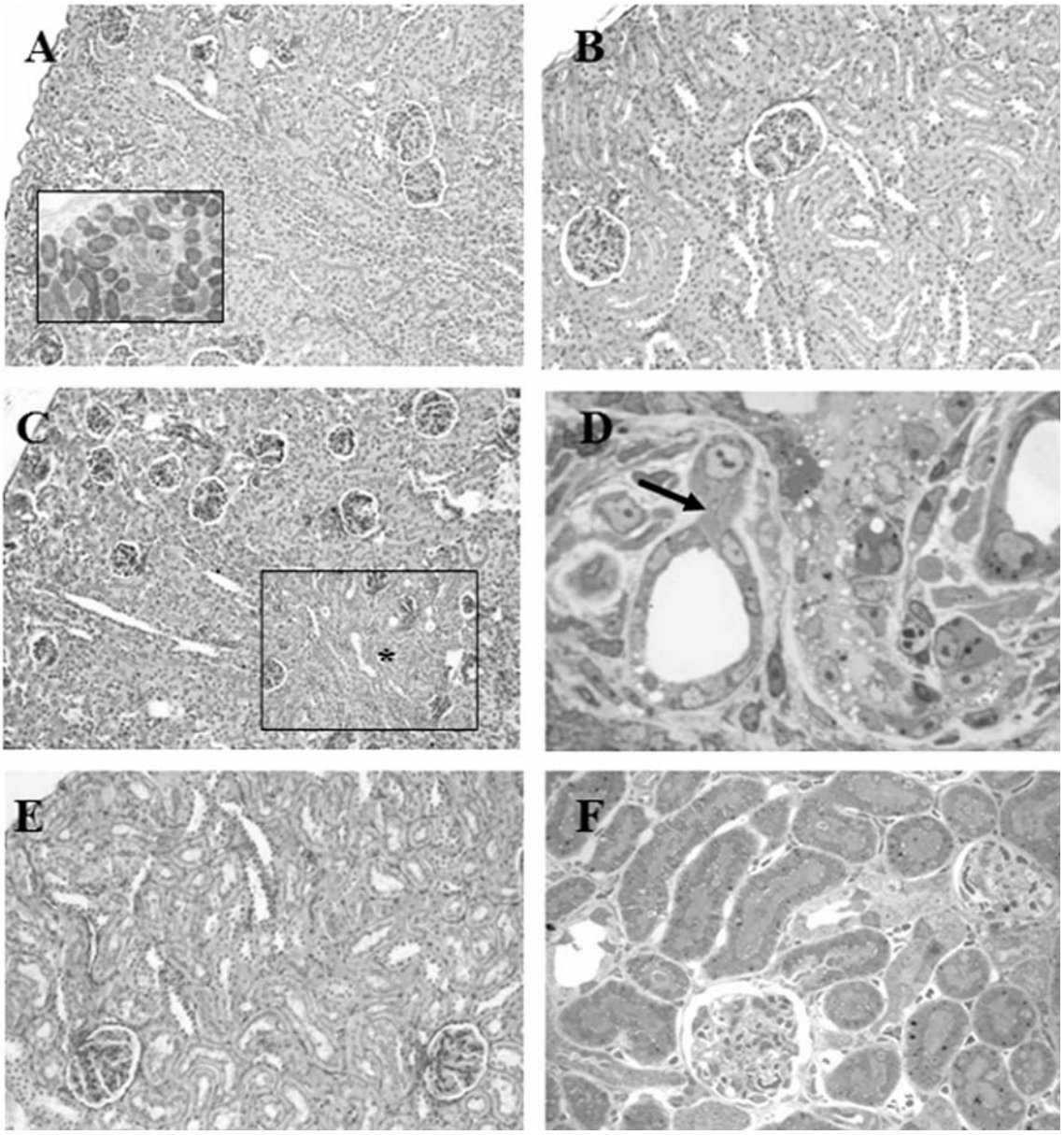

Figure 3. *Periodic Acid-Schiff (PAS) reaction, Toluidine Blue (TB) staining. Control kidney (A-B) and PtAcacDMS-treated samples (C-F). A. Nephrogenic areas in control neonatal kidney; B. Differentiated cortex at PD50. C. Neonatal PtAcacDMS-samples showing normal cortex and a fibrotic area at PD17 (asterisk, inset). D. Note the apparent migration of one epithelial cell (arrow) towards the peritubular interstitium within a fibrotic focus at PD17. E, F. Normal renal morphology of PtAcacDMS-samples at PD50. Original magnification: A, C ×20; A inset, B, E, F ×40; D ×100.*

considerable reduction in glomeruli number in cisplatin-treated samples compared to both control- and PtAcacDMS-treated samples (Figure 5). Differences between control animals and treated samples and between the two treated groups were statistically significant.

Immunoreactivity for E-cadherin. In control neonatal rat kidneys, strong E-cad immunoexpression labelled the epithelia of the medullary rays and their peripheral branches, the distal tubules and the macula densa, while proximal tubules were faintly stained (Figure 6A). In differentiated renal cortex of controls, the immunoreaction was restricted to the epithelia of the distal tubules and the macula densa and also that of the collecting ducts in a basolateral pattern (Figure 6B). At every stage, most medullary tubules showed moderate to intense E-cad positivity.

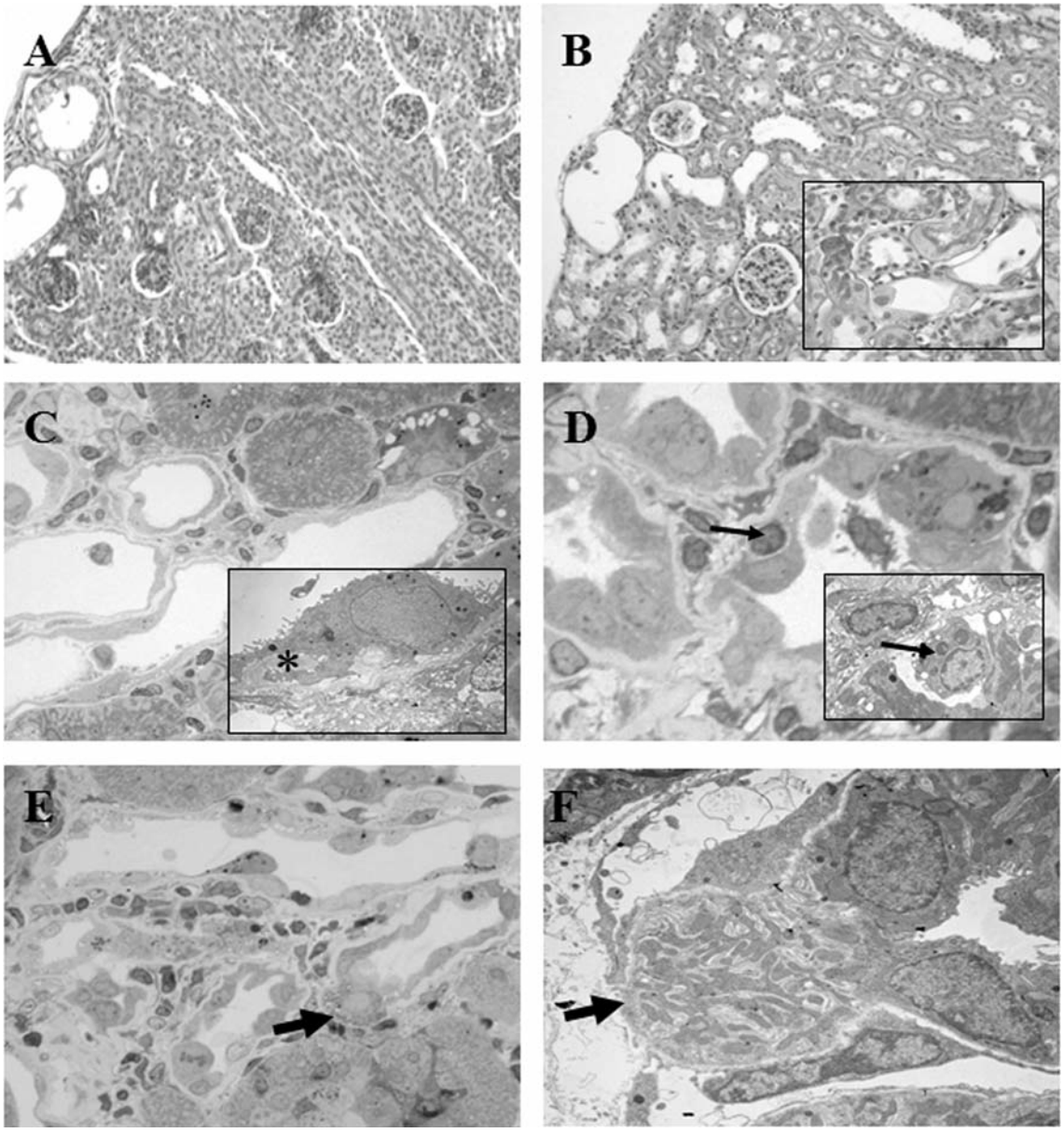

Figure 4. *Periodic Acid-Schiff (PAS) reaction, Toluidine Blue (TB) staining, ultrastructural images. Cisplatin-treated samples: newborn (A) and adult samples (B) showing altered tubules; in C a few tubules with flattened epithelia and thick basal lamina below (asterisk) are seen; in (D) tubule epithelia are surrounded by inflammatory cells; note an occasional infiltrating cells (thin arrows). In both (E) and (F) migrating epithelial cells towards the interstitium are visible (thick arrows); in (F) note interruption of the basal membrane. Original magnification: A, B ×20; C, D, E ×60; C, D insets, and F×3000.*

The pattern of E-cad labelling in the kidney of PtAcacDMS-treated rats generally appeared similar to control groups at every stage. Specifically, moderate to intense immunostaining was observed in several cortical tubules and medullary rays of neonatal rats (Figure 6C). In adults, the collecting duct segments and the medullary tubules displayed intense basolateral immunoreactivity (Figure 6D).

After treatment with cisplatin, the epithelia of numerous cortical and most medullary tubules of neonatal kidneys showed E-cad labelling. However, starting from PD17, some cortical tubules exhibited uneven positivity; among these, some tubules localized within a fibrotic area were also dilated (Figure 6E). In the adult samples, epithelia of certain tubules displayed heterogeneous E-cad expression in both

cortex and medulla. Most importantly, a number of cortical tubules with flattened epithelia did not show any evidence of E-cad (Figure 6F).

Immunoreactivity for vimentin. In control kidneys, peritubular interstitial cells, blood vessels and some glomerular cells -likely mesangial cells- were VIM-reactive. Compared to neonatal samples (Figure 7A), in adult samples peritubular VIM-labelling had diminished, especially in the cortex as compared to the medulla (Figure 7B).

The pattern of VIM labelling in the kidney of PtAcacDMS-treated rats generally appeared most similar to control groups at all stages. Along with glomeruli and vascular endothelia, intense VIM-positivity was typically apparent in mesenchymal cells of all renal zones at PD11 (Figure 7C) and PD17, declining in adult rats (Figure 7D). Rarely, tubule epithelia that reacted to VIM were seen within the cortex interspersed among the negative tubules at PD17 (Figure 7C) and in adult samples (Figure 7D); sporadic interstitial cells expressed VIM-positivity within the cortex of adults.

Compared to controls, within the renal parenchyma of cisplatin-treated samples remarkable changes were noted in the distribution of VIM-positivity from PD17 and culminating at PD50. In particular, at PD17, some VIM-immunoreactive tubules were noted within the cortex (Figure 7E); the VIM-labelled tubules were more numerous in the cortex of adult samples (Figure 7 F-H). In particular, at PD50 (Figure 7G), cortical dilated tubules were lined with flattened epithelia showing strong VIM expression; the more they exhibited a mesenchymal-like aspect the more they were reactive for vimentin. Occasional tubule epithelia showed a mosaic of VIM-positive and negative cells within the cortico-medulla (Figure 7H). Notable was a single spindle-shaped VIM-reactive cell observed in the act of detaching themselves from neighbouring epithelial cells (Figure 7F inset). Numerous reactive interstitial cells were seen close to altered tubules (Figure 7G).

Immunoreactivity for αSMA. In both controls (Figure 8A) and PtAcacDMS-treated neonatal rats (Figure 8C), an intense immunoreaction for αSMA labelled the interstitial cells in the renal parenchyma. Normally, peritubular αSMA disappeared and was no longer detectable in the cortex of control (Figure 8B) and PtAcacDMS-treated adult samples (Figure 8D), apart from very infrequent immunoreactive peritubular cells (Figure 8D inset). The glomeruli of the neonates weakly reacted to αSMA, while they showed no evidence of αSMA immunopositivity in all adult samples; blood vessels were reactive for αSMA in all samples.

After incubation for αSMA, some changes were detected when comparing neonatal cisplatin-treated samples with controls. As from PD17 (Figure 8E), and mainly in adult rats, moderate to intense αSMA-reactivity around some

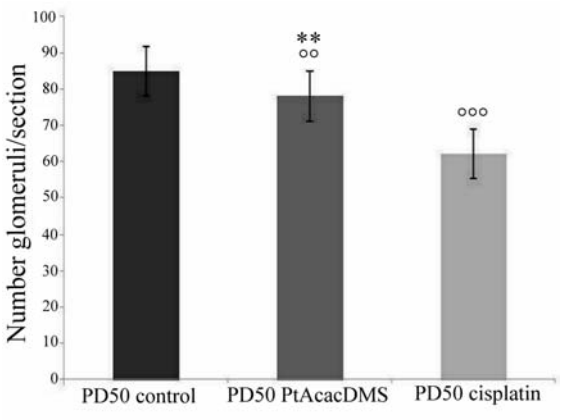

Figure 5. *Number of glomeruli in sections of controls and treated rats at PD50.*

tubules was observed in cisplatin-treated samples (Figure 8F, G and H) compared both to controls and PtAcacDMS-treated rats. Generally, at PD50, the pattern of immunoreactivity in the outer cortex consisted in intense peritubular staining all around a few injured dilated tubules with flattened epithelia (Figure 8 G and H).

Semi-quantitative evaluation of immunohistochemical stainings to E-cad, VIM and αSMA are summarized in Table I.

Discussion

Given that platinum derivative PtAcacDMS has been shown to perform a higher antitumor activity than cisplatin (15, 16, 23), we have dedicated the current study to compare both short and long-term nephrotoxic effects of a single dose of cisplatin vs. one of PtAcacDMS in rat kidney through histochemical analyses and certain immunohistochemical markers.

Our comparison between the differently treated groups and between these and control animals, besides the changes correlated to typical developmental processes (24), has evidenced a progressive renal tubulointerstitial fibrosis in cisplatin-treated rats, affecting in particular the outer renal cortex. Worthy of note was the correlation between histopathological changes and age, with alterations appearing more critical in adult rats than in neonatal ones, mainly after cisplatin treatment. Actually, in all adult rats treated with PtAcacDMS the occurrence of very few and restricted fibrotic lesions within regular cortex was the usual histological feature.

A significant finding was the reduced number of glomeruli recorded in adult cisplatin samples compared to those with PtAcacDMS, a likely result of incomplete nephron development after cisplatin dosage.

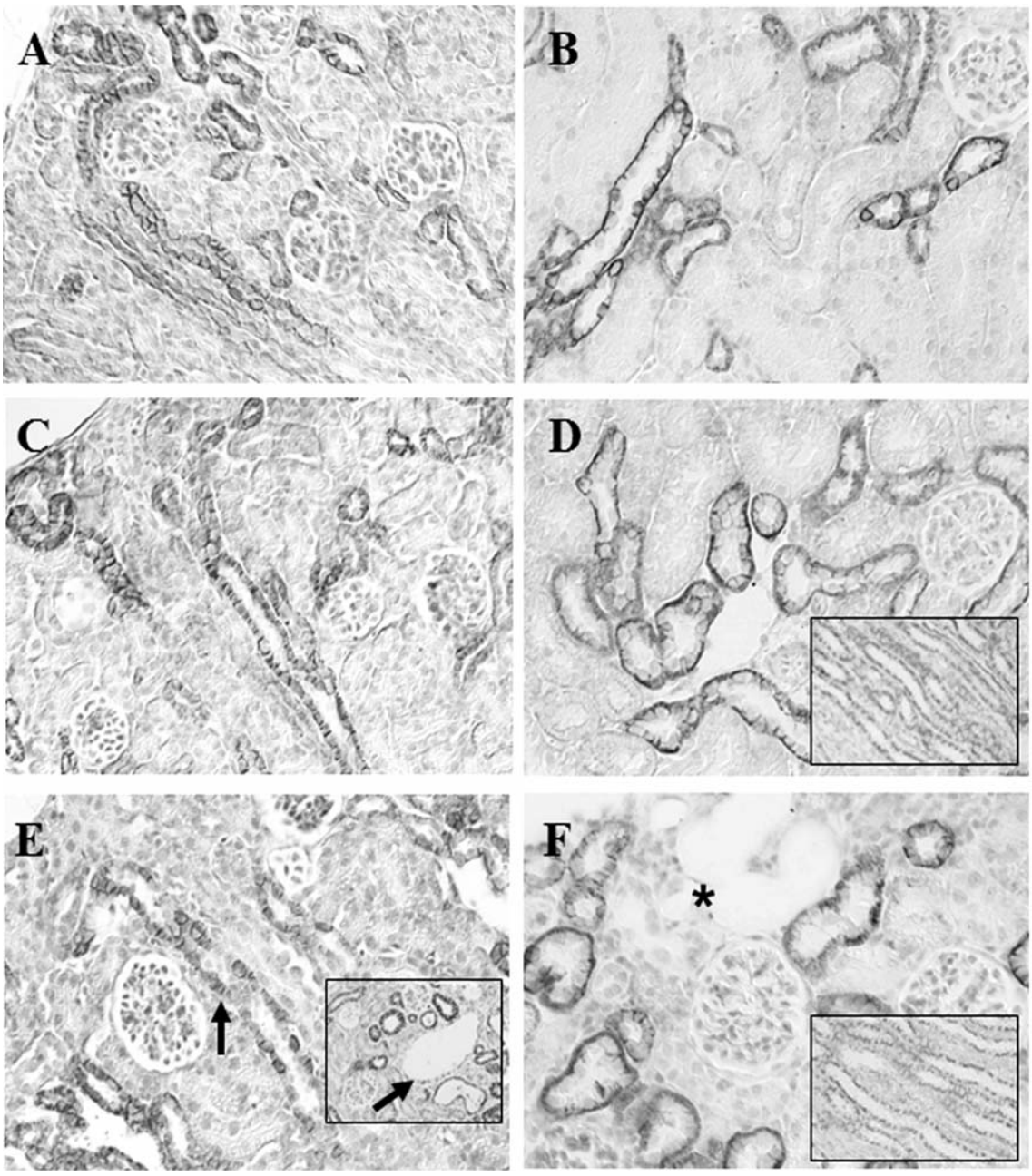

Figure 6. *Immunohistochemistry for E-cadherin. The epithelia of collecting ducts and distal tubules are reactive at the basolateral membranes in newborn controls (A) and in PtAcacDMS-samples (C); irregularly-stained tubule epithelia are visible in neonatal cisplatin-treated samples (E, arrows). Compared to adult control (B) and PtAcacDMS samples (D), in PD50 cisplatin-treated rats some cortical tubules are weakly-stained or totally negative (F, asterisk). Minor differences are observed by comparing medullary tubules of the two treated groups (D and F insets). Original magnification: A- F, ×40.*

In semi-thin sections of the treated samples, we detected tubulointerstitial changes confirming more severe fibrotic lesions in adult cisplatin-treated samples than in those treated with PtAcacDMS. Yet, we observed a remarkable event in two differently treated samples, namely, single cells exiting the confines of a tubule within a fibrotic lesion and migrating towards the neighbouring interstitium. This finding is of particular importance to the discussion on the role of EMT in renal fibrogenesis in light of the fact that some authors claim that no study has actually caught transformed epithelial cells

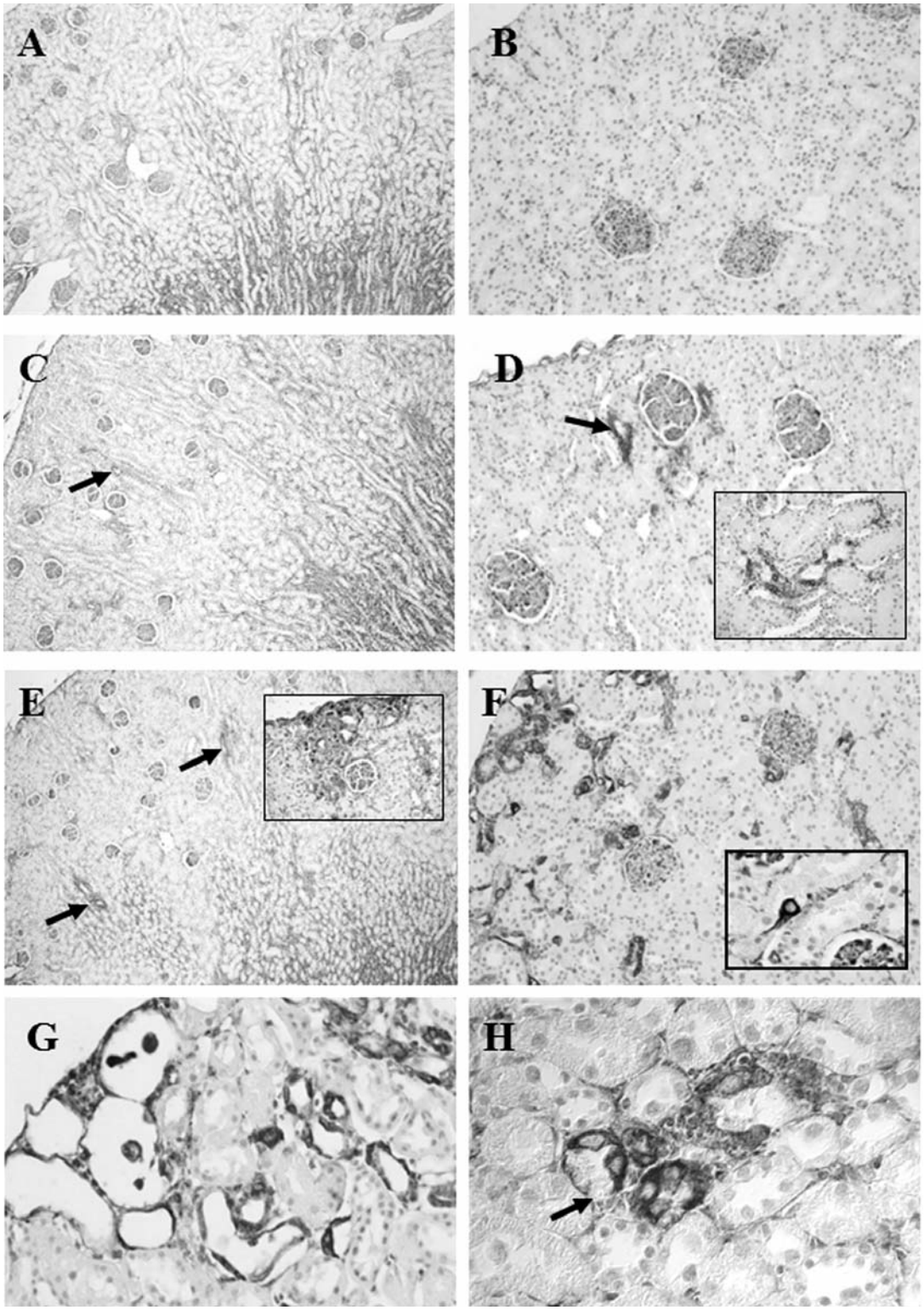

Figure 7. *Immunohistochemistry for vimentin. VIM expression is present in the interstitium, glomeruli and capillary endothelia of new-born (A) and adult control rats (B). Neonatal (C) and adult PtAcacDMS-treated samples (D) show sporadic VIM-positive tubule epithelia (arrows). In neonates a few cortical tubules are reactive after cisplatin-treatment (E). A number of reactive tubules are seen within the parenchyma of cisplatin-treated samples at PD31 (F) and PD50 (G, H). Note single migrating immunolabelled cells in F (inset). Original magnification: A, C, E, F ×20; B, D, E inset ×40; G, H, C and F inset, ×60.*

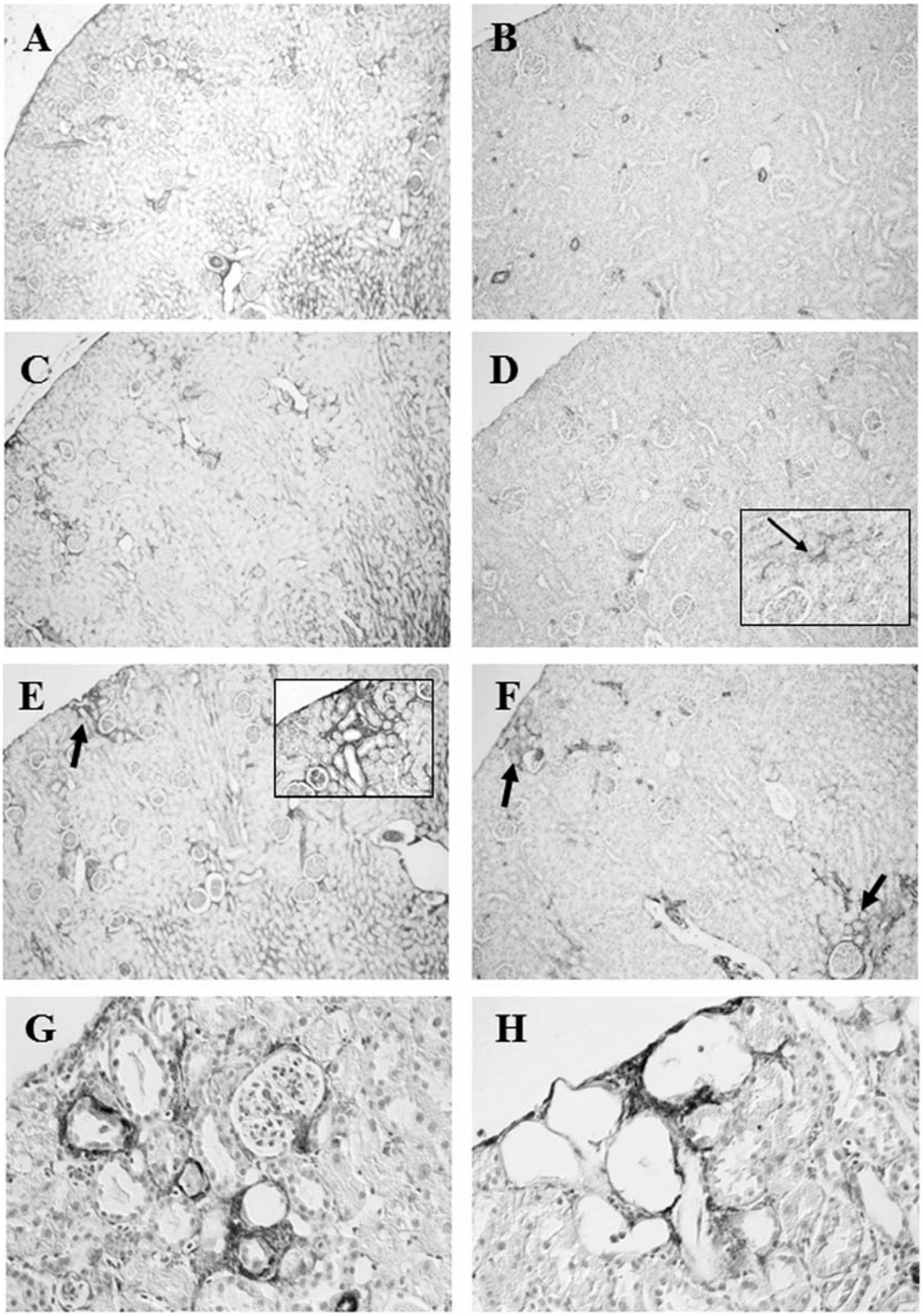

Figure 8. *Immunohistochemistry for αSMA. Peritubular interstitial staining is evident in neonatal control rats (A) and after PtACacDMS (C). In control (B) and PtAcacDMS (D) adults the reaction is decreased, except for small focal peritubular interstitium in PtAcacDMS adults (inset, arrow). In new-born cisplatin-treated samples dense focal αSMA deposits are present in nearby altered epithelia (E); in adult samples αSMA immunoreaction is evident encircling some tubules and glomeruli (F-H). In (H), strong reaction to αSMA around negative and dilated cortical tubules is observable. (Note that the same tubules express VIM-positivity in Figure 7G). Original magnification: A-E, B-F ×20; G, H ×60; D inset ×60; E inset ×40.*

Table I. *Immunohistochemical reactivity to E-cadherin (E-cad), vimentin (VIM), α smooth muscle actin (αSMA) in the renal cortex of control and treated rats.*

Antibody to		PD11		PD17		PD31		PD50	
	Groups	IC	EC	IC	EC	IC	EC	IC	EC
E-cad	Control	–	++/+++	–	++/+++	–	++/ +++	–	++/+++
	PtAcacDMS	–	++/+++	–	++/+++	–	++/+++	–	++/+++
	CisPt	–	++/+++	–	++/+++[a]	–	+/+++[a]	–	–, +/+++[a]
VIM	Control	++	–	++	–	+/–	–	+/–	–
	PtAcacDMS	++	–	++	+[b]	+/–	+[b]	+/–	+/++[b]
	CisPt	++	–	++	+/++[b]	+	+/++[b]	+	+/+++[a]
αSMA	Control	++	–	++	–	+/–	–	+/–	–
	PtAcacDMS	++	–	++	–	+/–	–	+	–
	CisPt	++	–	++	–	++[b]	–	++/+++[b]	–

IC, Interstitial cells; EC, epithelial cells. Scoring criteria as follows: –, negative; +/– very weak staining; +, weak staining; ++, moderate; +++, intense staining. [a]heterogeneous staining; [b]focal staining.

in the act of crossing the basal membrane into the interstitium (25-30). One exception does exist, however, in which the migration of a single epithelial cell, likely the intercalated cell of the collecting duct, was observed in a model of obstructed foetal-monkey kidney (31).

Besides histopathological findings, our immunohistological findings pose some interesting considerations on EMT and platinum-induced fibrogenesis.

EMT, first described as a process appearing during embryogenesis (32), is thought to be the key mechanism triggering tubulointerstitial fibrosis under certain pathological conditions (33-45).

In keeping with literature (46-48), we found in our control rats tubular E-cad immunopositivity primarily expressed at the basolateral membrane of adjacent epithelial cells of both collecting and distal tubules, while proximal tubules were negative. Accordingly, we considered those showing irregular E-cad reaction, present predominantly in cisplatin-treated rats, as damaged collecting tubules likely undergoing EMT. Interestingly, a few of them with cuboidal epithelia showed variable degrees of staining, while others, composed of fusiform-shaped cells, were completely negative for E-cad. Some studies suggest that, in pathological conditions, the reduction of E-cad, a transmembrane glycoprotein that is a typical marker of differentiated epithelia, is an early hallmark of EMT (49-52).

As regard the fibroblast markers -vimentin and αSMA- our findings on new-born and adult control rats demonstrated that gradual postnatal changes in the phenotype of cortical peritubular fibroblast parallel the functional maturation of tubular epithelia within the cortex in line with other reports (53-55). According to the aforementioned studies, intense interstitial cell expression of vimentin and αSMA have been associated with cell motility and the response to stretch and shearing forces accompanying nephrogenesis and tubular growth in the developing kidney.

Generally, our samples of neonatal rats treated with either of the platinum compounds were similar to the controls of the same age. However, starting from PD17, de novo expression of vimentin was evident in some tubule epithelia after both treatments. In cisplatin-treated animals, most epithelial cells showing VIM-positivity also exhibited fusiform mesenchymal-like morphology. Remarkably, while the amount of VIM immunolabelled tubules increased with the age of the rats in the majority of cisplatin-treated samples displaying damaged cortical areas, such staining was infrequent in adult PtAcacDMS-treated rats. Also based on our observations under the light microscope on semi-thin sections, it is likely that the majority of damaged tubules expressing intense vimentin are collecting ducts. This finding is not surprising considering that only epithelia in the collecting ducts show a transient expression of vimentin in developing kidneys, whereas it is not present in mature ones (56). Moreover, epithelia in the collecting ducts are particular prone to express this marker in response to fibrosis as reported in an *in vivo* (31) and in an *in vitro* study (57).

Concerning αSMA, unlike numerous reports demonstrating αSMA-positive epithelial cells in various *in vivo* models of kidney fibrosis in adult organisms, this study did not find any αSMA-reactive epithelia in any injured tubules at any time points. However, mainly after cisplatin treatment, αSMA-positive peritubular interstitium displaying variable intensity and thickness contoured damaged tubules.

Interestingly, recent studies suggest that EMT induces a variety of intermediate cell phenotypes, not all of which complete their transition to fibroblast (35, 58, 20). Accordingly, these intermediate cell phenotypes may be transient and

potentially reversible, thus allowing injured tubule cells to escape cell death and probably to repair damaged tubules if the inducer is removed. Moreover, Galichon *et al*. (59) suggest that EMT, also referred as "Epithelial Phenotypic Changes" (EPC), may reflect an exposure to a profibrotic environment, at an early and potentially reversible state.

Along with the histopathological findings, we found significant differences in kidney platinum content following the administration of the two platinum compounds: renal platinum content was higher after PtAcacDMS at each stage, at the same time that less serious nephrotoxicity was produced, even at PD50. The higher content of platinum found in kidney and brain (18) after PtAcacDMS fits with the data from *in vitro* studies on HeLa and MCF-7 cancer cells (15, 16) in which PtAcacDMS was taken-up at a higher rate and reached a nearly 10-times higher content than that of cisplatin. As the cytostatic effect of a platinum compound is directly related to its cell content, PtAcacDMS could have the considerable advantage of being used at a lower dose, thus reducing the risk of side-effects and drug resistance.

In conclusion, the present experimental model was proven suitable to investigate the occurrence of EMT in renal fibrogenesis. Besides the immunohistochemical results, the detection of occasional epithelial cells in the act of migrating to the interstitium in fibrotic areas, considering some authors' claims that there is no morphological recorded evidence of EMT involvement in fibrogenesis, is yet another important finding of this study. Finally, the present data, which confirm both our previous works demonstrating minor neurotoxic effects (17-19) and studies corroborating its remarkable antitumour activity and antimetastatic response (15, 16, 23, 60, 61), indicate that PtAcacDMS may be a potential alternative to the more toxic cisplatin.

Acknowledgements

This research was supported by a grant from the Fondazione Banca Monte Lombardia.

References

1 Shen DW, Pouliot LM, Hall MD and Gottesman MM: Cisplatin resistance: a cellular self- defense mechanism resulting from multiple epigenetic and genetic changes. Pharmacol Rev *64*: A-P, 2012.

2 Sànchez-Gonzàlez PD, Lòpéz-Hernandéz FJ, Lòpez-Novoa JM and Morales AI: An integrative view of pathophysiological events leading to cisplatin nephrotoxicity. Crit Rev Toxicol *4*: 803-821, 2011.

3 Han X, Yue J and Chesney RW: Functional TauT protects against acute kidney injury. J Am Soc Nephrol *20*: 1323-1332, 2009.

4 Appenroth D, Gambaryan S, Gerhardt S, Kersten L and Bräunlich H: Age dependent differences in the functional and morphological impairment of the kidney following cisplatin administration. Exp Pathol *38*: 231-239, 1990.

5 Yamate J, Machida Y, Ide M, Kuwamura M, Kotani T, Sawamoto O and Lamarre J: Cisplatin -induced renal interstitial fibrosis in neonatal rats, developing as solitary nephron unit lesions. Toxicol Path *33*: 207-217, 2005.

6 Ali BH, AL-Moundhri M, Tagedin M, Al Husseini IS, Mansour MA, Nemma A and Tanira MO: Ontogenic aspects of cisplatin -induced nephrotoxicity in rats. Food Chem Toxicol *46*: 3355-3359, 2008.

7 Espandiari P, Rosenweig B, Zhang J, Zhou Y, Scnackenberg L, Vaidya VS, Goering PL, BrownPP, Bonventre JV, Mahjoob K, Holland RD, Beger RD, Thompson K, Hanig J and Sadrieh N: Age-related differences in susceptibility to cisplatin -induced renal toxicity. Appl Toxicol *30*: 172-182, 2010.

8 Skinner R, Pearson ADJ, English MW, Price L, Wyllie RA, Coulthard MG and Craft AW: Cisplatin dose rate as a risk factor for nephrotoxicity in children. British J Cancer *77*: 1677-1682, 1998.

9 Skinner R, Parry A, Price L, Cole M, Craft AW and Pearson ADJ: Persistent nephrotoxicity during 10-year follow-up after cisplatin or carboplatin treatment in childhood: relevance of age and dose as risk factors. Eur J Cancer *45*: 3213-3219, 2009.

10 Dobyan DC: Long-term consequences of cis-platinum-induced renal injury: a structural and functional study. Anat Rec *212*: 239-245, 1985.

11 Yang T, Vesey DA, Johnson DW, Wei MQ and Gobe GC: Apoptosis of tubulointerstitial chronic inflammatory cells in progressive renal fibrosis after cancer therapies. Transl Res *150*: 40-50, 2007.

12 Kawai Y, Satoh T, Hibi D, Ohno Y, Kohda Y, Miura K and Gemba M: The effect of antioxidant on development of fibrosis by cisplatin in rats. Pharmacol Sci *111*: 433-439, 2009.

13 De Pascali SA, Papadia P, Ciccarese A, Pacifico C and Fanizzi FP: First examples of β-diketonate platinum II complexes with sulfoxide ligands. Eur J Inorg Chem *5*: 788-796, 2005.

14 De Pascali SA, Papadia P, Capoccia S, Marchiò L, Lanfranchi M, Ciccarese A and Fanizzi FP: Hard/soft selectivity in ligand substitution reactions of beta-diketonate platinum (II) complexes. Dalton Trans *37*: 7786-7795, 2009.

15 Muscella A, Calabriso N, De Pascali SA, Urso L, Ciccarese A, Fanizzi FP, Migoni D and Marsigliante S: New platinum (II) complexes containing both an O,O'-chelated acetylacetonate ligand and a sulfur ligand in the platinum coordination sphere induce apoptosis in HeLa cervical carcinoma cells. Biochem Pharmacol *74*: 28-40, 2007.

16 Muscella A, Calabriso N, De Pascali SA, Urso L, Ciccarese A, Fanizzi FP, Migoni D and Marsigliante S: (Pt(O,O'-acac) (γ-acac) (DMS)), a new Pt compound exerting fast cytotoxicity in MCF-7 breast cancer cells *via* the mitochondrial apoptotic pathway. Brit J Pharmacol *153*: 34-39, 2008.

17 Bernocchi G, Bottone MG, Piccolini VM, Dal Bo V, Santin G, De Pascali SA, Migoni D and Fanizzi FP: Developing central nervous system and vulnerability to platinum compounds. Chemother Res Pract *10*: 1155-1169, 2011.

18 Cerri S, Piccolini VM, Santin G, Bottone MG, De Pascali SA, Migoni D, Iadarola P, Fanizzi FP and Bernocchi G: The developmental neurotoxicity study of platinum compounds. Effects of cisplatin versus a novel Pt(II) complex on rat cerebellum. Neurotoxicol Teratol *33*: 273-281, 2011.

19 Piccolini VM, Bottone MG, Bottiroli G, De Pascali SA, Fanizzi FP and Bernocchi G: Platinum drugs and neurotoxicity: effects on intracellular calciun homeostasis. Cell Biol Toxicol *29*: 339-353, 2013.

20 Carew RM, Wang B and Kantharidis P: The role of EMT in renal fibrosis. Cell Tissue Res *347*: 103-116, 2012.
21 Bodenner DL, Dedon PC, Keng PC and Borch RF: Effect of diethyldithiocarbamate on cisdichlorodiammine-platinum (II)-induced cytotoxicity, DNA cross-linking and gamma-glutamyl transpeptidase inhibition. Cancer Res *46*: 2745-2750, 1986.
22 Raab A, Schat H, Meharg AA and Feldmann J: Uptake, translocation and transformation of arsenate and arsenite in sunflower (Helianthus annuus): formation of arsenic-phytochelatin complex during exposure to high arsenic concentrations. New Phytol *168*: 551-558, 2005.
23 Muscella A, Calabriso N, Vetrugno C, Urso L, Fanizzi FP, De Pascali SA and Marsigliante S: The signalling axis mediating neuronal apoptosis in response to (Pt(O,O'-acac) (γ-acac)(DMS)). Biochem Pharmacol *81*: 1271-1285, 2011.
24 Dressler GR: The cellular basis of kidney development. Ann Rev Cell Dev Biol *22*: 509-529, 2006.
25 Picard N, Baum O, Vogetsedre A, Kaissling B and Le Hir M: Origin of renal myofibroblasts in the model of unilateral ureter obstrution in the rat. Histochem Cell Biol *130*: 141-155, 2008.
26 Humphreys BD, Lin SL, Kobayashi A, Hudson TE, Nowlin BT, Bonventre JV, Valerius MT, McMahon AP and Duffield JS: Fate tracing reveals the pericyte and not epithelial origin of myofibroblasts in kidney fibrosis. Am J Path *176*: 85-97, 2010.
27 Barnes JL and Glass WF: Renal interstitial fibrosis: a critical evaluation of the origin of myofibroblasts. Contrib Nephrol *169*: 97-123, 2011.
28 Koesters R, Kaissling B, LeHir M, Picard N, Theilig F, Gebhardt R, Glick AB, Hahnel B, Hosser H, Grone HJ and Kriz W: Tubular overexpression of transforming growth factor-1 induces autophagy and fibrosis but not mesenchymal transition of renal epithelial cells. Am J Path *177*: 632-643, 2010.
29 Kritz W, Kaissling B and Le Hir M: Epithelial-mesenchymal transition (EMT) in kidney fibrosis: fact or fantasy? J Clin Invest *121*: 468-474, 2011.
30 Grgic I, Duffield JS and Humphreys BD: The origin of interstitial myofibroblasts in chronic kidney disease. Pediatr Nephrol *2*: 183-193, 2012.
31 Butt MJ, Tarantal AF, Jimenez DF and Matsell DG: Collecting duct epithelial–mesenchymal transition in fetal urinary tract obstruction. Kidney Int *72*: 936-44, 2007.
32 Greenburg G and Hay ED: Epithelia suspended in collagen gels can lose polarity and express characteristics of migrating mesenchymal cells. J Cell Biol *95*: 333-339, 1982.
33 Iwano M, Plieth D, Danoff TM, Xue C, Okada H and Neilson EG: Evidence that fibroblasts derive from epithelium during tissue fibrosis. J Clin Invest *110*: 341-350, 2002.
34 Liu Y: Epithelial to mesenchymal transition in renal fibrogenesis: pathologic significance, molecular mechanism, and therapeutic intervention. J Am Soc Nephrol *15*: 1-12, 2004.
35 Liu Y: New insights into epithelial-mesenchymal transition in kidnew fibrosis. J Am Soc Nephrol *21*: 212-222, 2010.
36 Vongwiwatana A, Tasanarong A, Rayner DC, Melk A and Halloran PF: Epithelial to mesenchymal transition during late deterioration of human kidney transplants: the role of tubular cells in fibrogenesis. Am J Transplant *5*: 1367-1374, 2005.
37 Strutz F and Muller GA: Renal fibrosis and the origin of the renal fibroblast. Nephrol Dial Transplant *21*: 3368-3370, 2006.
38 Acloque H, Adams MS, Fishwick K, Bronner-Fraser M and Nieto MA: Epithelial mesenchymal transition: the importance of changing cell state in development and disease. J Clin Invest *119*: 101-104, 2009.
39 Efstratiadis G, Divani M, Katsioulis E and Vergoulas G: Renal fibrosis. HIPPOKRATIA *13*: 24-28, 2009.
40 Kalluri R and Weinberg RA: The basics of epithelial-mesenchymal transition. J Clin Invest *119*: 1420-1428, 2009.
41 Carvallo de Matos AC, Saraiva Camara NO, Tonato EJ, de Souza Durao M, Franco MF, Ribeiro Moura LA and Pacheco-Silva A: Vimentin expression and myofibroblast infiltration are early markers of renal dysfunction in kidney transplantation: an early stage of chronic allograft dysfunction? Transpl Proc *42*: 3482-3488, 2010.
42 Zeisberg M: Resolved: EMT produces fibroblasts in the kidney. J Am Soc Nephrol *2*: 1247-1253, 2010.
43 Frangiadaki M and Mason RM: Epithelial-mesenchymal transition in renal fibrosis –evidence for and against. Int J Exp Path *92*: 143-150, 2011.
44 Galichon P and Hertig A: Epithelial to mesenchymal transition as a biomarker in renal fibrosis: are we ready for the bedside? Fibrogen Tissue Repair *4*: 11-21, 2011.
45 Kim MK, Maeng Y, Sung WJ, Oh HK, Park JB, Yoon GS, Cho CH and Park KK: The differential expression of TGF-β1, ILK and wnt signalling inducing epithelial to mesenchymal transition in human renal fibrogenesis: an immunohistochemical study. Int J Clin Exp Pathol *6*: 1747-1758, 2013.
46 Cho EA, Patterson LT, Brookhiser WT, Mah S, Kintner C and Dressler GR: Differential expression and function of cadherin-6 during renal epithelium development. Development *125*: 803-812, 1998.
47 Prozialek WC, Lamar PC and Appelt DM: Differential expression of E-cadherin, N-cadherin and beta-catenin in proximal and distal segments of the rat nephron. BMC Physiol *4*: 1-14, 2004.
48 Shen SS, Krishna B, Chirala R, Amato RJ and Truong LD: Kidney-specific cadherin, a specific marker for the distal portion of the nephron and related renal neoplasms. Mod Pathol *18*: 933-940, 2005.
49 Aresu L, Rastaldi MP, Prege P, Valenza F, Radaelli E, Scanziani E and Castagnaro M: Dog as model for down-expression of E-cadherin and beta-catenin in tubular epithelial cells in renal fibrosis. Virchows Arch *453*: 617-625, 2008.
50 Thiery JP, Acloque H, Huang RYJ and Nieto A: Epithelial-mesenchymal transitions in development and disease. Cell *139*: 871-890, 2009.
51 Veerasamy M, Nguyen TQ, Motazed R, Pearson AL, Goldschmeding R and Dockrell ME: Differential regulation of E-cadherin and alpha-smooth muscle actin by BMP 7 in human renal proximal tubule epithelial cells and its implication in renal fibrosis. Am J Physiol Renal Physiol *297*: 1238-1248, 2009.
52 Zheng G, Lyons JG, Tan TK, Wang Y, Hsu TT, Min D, Succar L, Rangan GK, Hu M, Henderson BR, Alexander SI and Harris DC: Disruption of E-cadherin by matrix metalloproteinase directly mediates epithelial-mesenchymal transition downstream of transforming growth factor-beta1 in renal tubular epithelial cells. Am J Pathol *175*: 580-591, 2009.
53 Marxer-Meier A, Hegyi I, Loffing J and Kaissling B: Postnatal maturation of renal cortical peritubular fibroblasts in the rat. Anat Embryol *197*: 143-153, 1998.
54 Kaissling B and Le Hir M: The renal cortical interstitium: morphological and functional aspects. Histochem Cell Biol *130*: 247-262, 2008.

55 Yuasa T, Izawa T, Kuwamura M, Yamate J: Thy-1 expressing mesenchymal cells in rat nephrogenesis in correlation with cells immunoreactive for α –smooth muscle actin and vimentin J Toxicol Pathol *23*: 1-10, 2010

56 Holthöfer H, Miettinen A, Lehto VP, Lehtonen E and Virtanen I: Expression of vimentin and cytokeratin types of intermediate filament proteins in developing and adult human kidneys. Lab Invest *50*: 552-559, 1984.

57 Ivanova L, Butt MJ and Matsell DG: Mesenchymal transition in kidney collecting duct epithelial cells. Am J Physiol Renal Physiol *294*: 1238-1248, 2008.

58 Zeisberg M and Neilson EG: Mechanisms of tubulointerstitial fibrosis. J Am Soc Nephrol *21*: 1819-1834, 2010.

59 Galichon P, Finianos S and Hertig A: EMT-MET in renal disease: should we curb our enthusiasm? Cancer Letters *341*: 24-29, 2013.

60 Muscella A, Vetrugno C, Migoni D, Biagioni F, Fanizzi FP, Fornai F, De Pascali SA and Marsigliante S: Antitumor activity of (Pt(O,O'-acac)(c-acac)(DMS)) in mouse xenograft model of breast cancer. Cell Death Dis *5*: e1014, 2014.

61 Vetrugno C, Muscella A, Fanizzi FP, Cossa LG, Migoni D, De Pascali SA and Marsigliante S: Different apoptotic effects of (Pt(O,O'-acac)(γ-acac)(DMS)) and cisplatin on normal and cancerous human epithelial breast cells in primary culture. Br J Pharmacol *171*: 5139-5153, 2014.

Received October 15, 2014
Revised November 4, 2014
Accepted November 7, 2014